Please use this template and for submitting a new or revised manuscript to any AGU journal. Using this template and following the guidelines below will help us expedite processing of your paper.

The template starts on page 2. Delete this cover page.

Helpful links:

Descriptions of individual journals and links to their submission sites are here: https://www.agu.org/Publish-with-AGU/Publish

Additional instructions are available under "How to Submit" in the link above.

Please follow our checklists for initial submission or revision**. Resubmissions that were previously reviewed should follow the "revision" checklist.**

AGU has implemented new styles. These mostly affect formatting of references, which are now cited in parentheses, not brackets. See here for details.

Length: Research Articles in most AGU journals have an allowed length of 25 publication units. Letters in *Geophysical Research Letters (GRL)* and Technical Reports on Data or Methods in *Earth and Space Science* have an allowed length of 12 publication units (1 unit = 500 words or 1 table or figure; title, plain language summary, author lists, references, and all supplements are excluded from the word count).

AGU encourages research publications that are thorough but also concisely presented. This benefits readers as well as reviewers, who are increasingly taxed. Editorial and production costs also scale with length. However, all AGU journals except *GRL* allow longer papers beyond these guidelines for an additional fee (**see table**) that reflects these incentives. ***Submissions to GRL that are longer than the allowed length of 12 Publication Units will be returned immediately for shortening.*** Some journals have publication fees. Open access is available in all AGU journals.

Please use the .docx format if possible (all versions of Word after 2007). This document contains pre-set styles that apply to each manuscript element. These styles are listed below. Please keep these styles by pasting in your text when done and matching, or applying these styles in your document using the style pane or organizer.

Title

Authors

Affiliation

Key points

Abstract

Plain Language Summary

Body Text

Headings (Main and secondary)

Figure or Table Captions

References

Please use our separate template for supporting information: https://www.agu.org/-/media/Files/Publications/AGUSupporting-Information_Word_template.docx?la=en&hash=BEA4EB05F3A8E5C18A2BAAC5BCCDBC9E33FFBC25

More specific formatting instructions are provided in the actual template, which follows. Delete these instructions from your finished manuscript.

AGU requires the corresponding author to register for an ORCID. Co-authors are also encouraged to register. We will note published contributions and reviews in your ORCID profile. Each author can easily create or link your ORCID in GEMS via Modify Profile/Password on the landing page.

Remote sensing scale effect in urban karstic terrain runoff modeling

Y.Anker [1 2 †] *, N. Ne'eman [3 †], I. Benenson [4 †]

[1] The Department of Chemical Engineering, Ariel University, Ariel, 40700, Israel

[2] The Department of Environmental Research, Eastern R&D Center, Ariel, 40700, Israel

[3] The Department of Environmental Engineering, School of Engineering, Tel Aviv University, 69978, Israel

[4] The Department of Geography and Human Environment, Porter School of Environment and Earth Sciences, Faculty of Exact Sciences, Tel Aviv University, 69978, Israel

Corresponding author: Yaakov Anker (kobia@Ariel.ac.il)

[†]Yaakov Anker, Nitzan Ne'eman and Itzhak Benenson contributed equally to this article.

Key Points:

- Optimal resolution for urban watershed grid-based model was of four meters, as a lower resolution is insufficient and a higher resolution is redundant.
- Besides saving computer resources, lower resolution acts as a smoothing filter for minor structural elements that do not influence real-world hydrology.
- The strategy presented, was able to correctly model urban runoff in mountainous karstic terrain.

Abstract

Urbanization tends to increase runoff volumes, which might cause flooding and reduce groundwater recharge. Since the design of impermeable urban elements is based on the water flow volume before their construction, once they are erected the induced change to the local drainage pattern might generate flooding of the newly developed and previously developed areas. As such, precise modeling is essential to allow municipal watershed sensitive hydrological design, which may prevent impervious urban surface expansion negative impacts. Digital elevation model that represent the watershed relief at any given location is the hydrological modeling base layer, which is necessary for describing urban landscapes and watersheds. The common notion is that the finer the elevation model resolution is, the more precise the hydrological model will be. Nevertheless, it is suggested that over-accuracy might be redundant. In the same manner, the land use classification resolution should be aligned with the modeling requirements. Such careful evaluation of the modeling resolution will reduce the computing resources needed for the modeling procedure and may be utilized as a sensitivity filter for insignificant tributaries of the hydrological network. This paper demonstrates a nominal procedure for urban watershed sub-basin analysis, which is the initial stage for detailed urban runoff modeling. It was found that the scale-optimized model performed very well and was found suitable for the prediction of runoff volume and discharge from a mainly urban, mountainous karstic watershed.

Plain Language Summary

The development of modern cities tends to expand areas of roads, parking lots, rooftops, sidewalks and other manmade elements. These impermeable surfaces prevent rainwater percolation to the ground and increase the water flow volume on and from these areas, which might cause resident area flooding. To prevent such a scenario it is essential to anticipate the surplus water flow volumes at the city or neighborhood scale, taking into mind the future infrastructure development. The common tool enabling such a prediction is runoff modeling over a computerized geographic information system, which may provide drainage engineers, with the correct water volumes and flow intensities for future drainage design. While for similar precipitation coverage and urban development plan, homogenous areas modeling requires merely the area averaged infiltration rate, in heterogenous areas a distributed modeling that adjust a specific infiltration coefficient to various sub-sections of the area is required. This study simulated the quantities and flow velocities of runoff generated by rainfall over a karstic (weathered dolostone terrain) peri-urban drainage basin. By applying differential infiltration coefficient and optimal resolution scale, the model that was developed for the region was able to correctly simulate the runoff produced by several rainstorms.

1 Introduction

Urban areas are characterized by impervious surfaces such as roads, sidewalks, parking lots and buildings covering vast areas. These surfaces prevent rainfall infiltration into the ground. In addition, the natural flow paths are replaced by paved gutters, storm sewers, or other elements of artificial drainage. As a

result, cities generate increased runoff volumes with increased peak discharges and shorter travel times compared to the pre-urbanized state As cities constantly grow, more and more areas are changed from natural to urban. Precise modeling is required to allow an urban drainage system designed (of overland flow paths and underground pipes) to cope with the additional discharge that otherwise will overflow and flood roads, houses, parks, etc. [*Gao et al.*, 2021].

Runoff is the surface flow of the excess rainfall that did not infiltrate the ground or evaporate. Rainfall-runoff models are mathematical models that compute surface runoff in response to a rainfall input and are an applicative tool for estimating runoff discharge and total volume, both from natural and urban watersheds [*Fletcher et al.*, 2013]. A drainage watershed is an area of land, which is drained into a single point at a lower elevation that is called the watershed's outlet. A watershed may be of any size and can include secondary watersheds (sub-watersheds), which are defined by secondary outlets [*McCuen M.*, 2004]. Urban watershed land use has the greatest impact on surface runoff initiation by dictating the evapotranspiration and soil coverage degree [*Fohrer et al.*, 2001]. Urbanization tends to enlarge impervious surfaces such as roads, sidewalks, parking lots and buildings, which cover previously natural permeable areas. Moreover, the modification of natural flow paths into paved gutters, storm sewers, or other artificial drainage elements changes the overall watershed's response to precipitation such that developed urban watersheds generate increased runoff volumes, with increased peak discharges. Runoff that travels faster to the watershed's outlet might cause flooding once the watercourse slope moderates [*Anker et al.*, 2019].

Urban watersheds have very heterogenic land uses with typical variation in the scale of a few meters, whereas in natural watersheds the typical variation of the watershed's characteristics is over a larger scale (tens or hundreds of meters). Therefore, an urban rainfall-runoff model requires as input a representation of the watershed's impervious and pervious areas, and more specifically a Land-Use Classification [*McCuen M.*, 2004]. Surface topography is represented in Geographical Information Systems (GIS) by a Digital Elevation Model (DEM) which is derived using an interpolation of known elevation points and their locations. DEM is commonly presented using a raster data file (a form of grid dataset) where each cell contains an elevation value. The raster's cells can be of any size, usually ranging from a few meters to a few kilometers. Determining the raster's cell size is dependent on available data, watershed scale, and considerations such as computation time, which increases as the resolution increases. DEMs are frequently employed to derive basic topographic characteristics, thanks to the incorporation of numerous algorithms into commercial or public license GIS; e.g., [*Greenlee*, 1987; *Jenson and Domingue*, 1988; *Hutchinson*, 1989; *Tarboton et al.*, 1991].

Land Use classification may be performed using Remote Sensing techniques based on satellite images or aerial photos, which also supplies information regarding its spatial distribution within the watershed, dictating the runoff volumes

that reach the watershed and the concentration-time [*Olivera and Maidment*, 1999]. Existing land use data varies in the level of accuracy and resolution. The United States Geological Survey (USGS) Land Cover Institute (LCI) has a free Land Use / Land Cover (LU/LC) database with a maximum resolution of 30-m. In Israel, the Central Bureau of Statistics offers a public-free nationwide vector LC/LU classification. However, these classifications are composed of lumped (aggregated) classes such as "urban areas" or "industrial areas", without separation to impervious and pervious surfaces and their specific land cover. Thus, this general classification could not be used in a distributed urban runoff model [*Jacqueminet et al.*, 2013].

This paper evaluates the optimal spatial scale for a spatially distributed high-resolution Rainfall-Runoff model implementation in a mountainous karst urban watershed. More explicitly, this work:

- evaluates several spatial resolutions, to obtain the optimal resolution that will represent the watershed's characteristics in a nominal grid-based classification.

- validates that the Digital Elevation Model (DEM), generated by this optimal resolution, represents a hydrologically correct sub-basin analysis.

2 Methodology

Mountainous karst urban watersheds are probably the most complicated scenario for hydrological modeling. To develop a methodology of a spatially distributed high-resolution Rainfall-Runoff model that can handle such a terrain the study site should be equipped with a monitoring system capable of measuring sufficient components of the hydrological system. The city of Ariel's geological infrastructure consists of fractured limestone and dolostone with karstic features [Litvak et al., 2018]; it is also equipped with a hydrological monitoring system that was constantly operated for six years before this study.

2.1. Study area

The city of Ariel is located on the Samaria Mountain range in Israel, in the area which is referred to as the Jordan River Western Bank. It is within the Yarkon-Ayalon 1800 km^2 watershed that is one of the largest watersheds in Israel, with its surface datum the Mediterranean Sea. The flow path runs through the narrow outlet of the Yarkon River, which is located in the very center of Israel's largest metropolitan area [*Ne'eman*, 2015] The mountain range is composed of Terra Rossa and Rendzina soils on top of hard limestone and dolomite [*Dan et al.*, 1995]. This mountain range serves as the recharge zone of the Mountain Aquifer, which is Israel's most important water resource both in quantity and quality aspects [*Gvirtzman*, 2002]. The total size of Ariel's urban watershed is 1.9 km^2, which is defined as the outlet at the southwest point on the ephemeral stream (wadi) that crosses the city (Figure 1). Ariel sprawls over a few mild hills and the wadi between them, with a maximal elevation of 702 mASL and a minimum elevation of 509 mASL.

The storm-water gravitational drainage network is designed according to the

city's topography. Information regarding the drainage system's pipes' location, dimensions, and connectivity are not properly documented and is considered altogether missing. However, it is assumed that it is situated in high correlation to the topography. In addition, it is known that the drainage network has a few outlets where it discharges the collected runoff from higher parts of the city into a lower wadi, which serves as a city park with a stream in its midst. The park stream serves as a central flow path of the watershed.

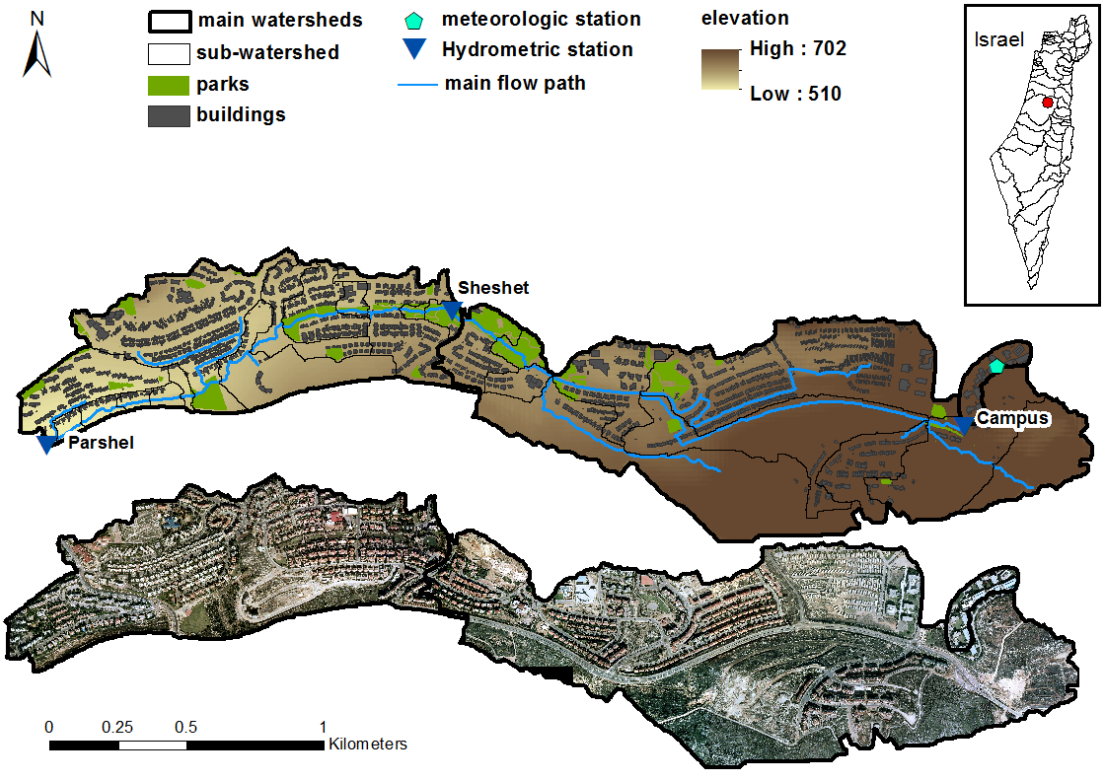

Figure 1: Below: Ariel air-photo and main sub-watersheds. Above: Ariel watershed's general topography, built-up areas, parks, and the main flow path through the city.

2.2. Digital Elevation Model (DEM)

To represent an urban surface small-scale variation, an accurate DEM is required. While many studies suggested that DEM quality and resolution significantly affect the accuracy of any extracted hydrological parameter [*Kenward et al.*, 2000], some studies indicated that too high a resolution might create chaotic flow patterns, which can be avoided by reducing DEM resolution from centimeters to up to meters *[Blackwell and Wells,* 1999*]*. Vaze et al. (2010) analyzed and compared a high-resolution 1-meter LIDAR DEM to a 25-meter Cartographic DEM, both re-sampled to various resolutions. They indicated that the input

DEM resolution accuracy has severe implications on the derived hydrologically spatial properties Another method for elevation mapping is LIDAR, remote sensing (RS) technique that measures distance by illuminating the target with a laser and analyzing the reflected light. LIDAR has a very high sampling density, which produces very high-resolution DEMs of less than 1 meter [*Murphy et al.*, 2008]. Although LIDAR has advantages for urban hydrology models, it is still not commonly available owing to high costs and massive processing resources. For this reason, other DEMs such as high-resolution photogrammetric DEMs are commonly used. Nevertheless, even high-resolution DEMs with a resolution of a few meters might be insufficient to capture the fine urban topography.

Thus, other techniques for re-processing and correcting available DEMs are commonly used for deriving a DEM that can represent an urban watershed's hydrologic properties. A common processing technique is enforcing the known flow paths by artificially reducing the DEM cell elevation by a specified height. This is done to make sure that they are lower than their surroundings, as in reality. This technique, which is also known as "DEM burning", has been used in numerous studies and proved to improve hydrology property derivation; e.g., [*Murphy et al.*, 2008]-[*Gironás et al.*, 2010]-[*Hankin et al.*, 2008]-[*Lhomme et al.*, 2004]-[*Mark et al.*, 2004]-[*Rodriguez et al.*, 2000]-[*Zech et al.*, 1994]

In this study, a high-resolution DEM was created based on photogrammetric-derived contours with a vertical interval of 0.5 meters. The DEM was generated using ArcGIS's Topo To Raster tool, an interpolation method specifically designed for the creation of hydrologically correct DEM. The Topo To Raster algorithm allows for the inclusion of streamlined data, which are used to ensure that each stream lies at the bottom of its valley. Once an initial DEM is derived using the Topo to Raster tool, the contours and height points are inserted into the tool as contours and elevation points, respectively, and the roads and culverts are inserted as streams. Then, the streets and culverts that serve as flow paths in the watershed are "burnt" into the resulting DEM, in a factor of twice the cell size [*Hutchinson*, 1989]. This DEM shows the natural topography of Ariel, without the effect of urban features. The DEM was corrected using the city engineering department's measurement data of road slopes and other flow paths, and also by applying field survey data on culvert locations. An analysis was made to determine the minimum necessary resolution for correctly delineating the urban watershed's flow paths and sub-basin boundaries.

2.3 Land Use/land-cover Classification

Medium resolution orbital sensors such as Landsat Thematic Mapper (TM) (at 30 m pixel resolution) and SPOT High-Resolution Visible (HRV) (at 20 m) are commonly classified for land covers in many studies [*Jacobson*, 2011]. However, as it is not possible to distinguish features with dimensions smaller than the pixel resolution, the resolutions of these sensors restrict their use in urban watersheds [*Anker et al.*, 2014]. An alternative is supplied by high-resolution imagery such as an orthophoto. Having pixel size as small as 0.5 meters, an orthophoto is capable of providing greater detail in complex urban areas and has been used

successfully in some studies. Branger et al. (2013) and Jacqueminet et al. (2013) explored the potential of very high-resolution (VHR) optical images (0.5–2.5 m) for retrieving LU/LC information for distributed hydrological models, concluding that for models of watersheds in the scale of a few km^2, manual digitizing based on the 0.5 m resolution image was found to be the most accurate to provide the required information. It allowed the retrieval of valuable information about natural and impervious areas, hedgerows, vegetation type and rotation and bare soils, and greatly improved the model parameterization. However, manual digitizing is time-consuming and quite slow.

A very high resolution (0.2 m) RGB orthophoto of the study area, taken in 2006, was classified into five LUs. Since in three bands different LU may have a similar visible spectrum, a Feature-Based classification was implemented. The image analysis software ENVI's Feature Extraction module extracts information from high-resolution imagery based on spatial, spectral and textural characteristics. The ENVI Feature Extraction module uses an object-based approach to classification, as opposed to traditional pixel-based classification. The benefit of an object-based approach is that it allows objects to be classified also according to their shape and size in addition to spectral and textural characteristics.

The orthophoto tiles are enhanced using Histogram Matching and Histogram Stretching techniques and are mosaicked into a single image. To overcome the issue of shades in the image resulting from buildings and trees, the shaded area is masked and then classified separately from the rest of the image.

The feature extraction process starts with Segmentation, which is the process of partitioning an image into segments by grouping neighboring pixels with similar feature values (brightness, texture, color, etc.). These segments ideally correspond to real-world objects. The edge-based segmentation algorithm has a single Scale Level parameter ranging from 0 to 100, with high values for coarse segmentation and low values for fine segmentation. The Merging process is an additional optional step used to aggregate small segments within larger, textured areas such as trees or fields. The Merge Level parameter represents the threshold lambda value [*Jiao et al.*, 2012], which also ranges from 0 to 100, where low values may result in over-segmenting and high values in under-segmenting.

2.4. Methodology of model evaluation

The Nash and Sutcliff coefficient of Efficiency (NSE, Eq. 1) is used to evaluate hydrologic model performance [*Nash and Sutcliffe*, 1970; *Legates and McCabe*, 1999]. This efficiency coefficient ranges from minus infinity to 1.0, with higher values indicating better agreement:

$$NSE = 1 - \frac{\sum_{i=1}^{N}(O_i - P_i)^2}{\sum_{i=1}^{N}(O_i - \overline{O})^2} \quad \textit{Eq. } \mathbf{1}$$

where O_i is the observed discharge in time increment i, P_i is the predicted model

simulation discharge in time increment i and $\overline{O}$ is the mean of observed discharge and N is the last time increment.

Physically, NSE is the ratio of the Mean Square Error (MSE) (Eq. 2) to the variance in the observed data, subtracted from unity.

$$MSE = N^{-1} \sum_{i=1}^{N} (O_i - P_i)^2 \quad Eq.\ 2$$

Thus, if the square of the differences between the model simulation and the observations is as large as the variability in the observed data, then NSE = 0, and if it exceeds it, then NSE < 0.

Thus, NSE = 0 indicates that the observed mean is as good a predictor as the model, while NSE < 0 indicates that the observed mean is a better predictor than the model (both are unacceptable results). NSE = 1 is a perfect fit, while NSE > 0.5 is considered a satisfactory model performance [*Moriasi et al.*, 2007].

Another acceptable statistical indicator is the Percent Bias (referred to in this study as Deviation Percent). Deviation Percent measures the average tendency of the simulated data to be larger or smaller than their observed counterparts [*Gupta et al.*, 1999]. The optimal value of Deviation percent is 0.0, with low-magnitude values indicating accurate model simulation. Positive values indicate model overestimation bias, and negative values indicate model underestimation bias. Deviation percent (D%) is calculated with equation 3:

$$D\% = \frac{\sum_{i=1}^{n} \left(Y_i^{\mathrm{sim}} - Y_i^{\mathrm{obs}}\right)}{\sum_{i=1}^{n} Y_i^{\mathrm{obs}}} * 100 \quad Eq.\ 3$$

where Y_i^{obs} indicates the observed model element in time i, and Y_i^{sim} indicates the simulated model element in time i.

Moriasi et al. [2007] gave general performance ratings for the NSE and Deviation Percent, which are summarized in Table 1.

Table 1: General performance ratings for recommended statistics indicators

Performance Rating	**NSE**	**Deviation Percent (D%)**
Very Good	0.75 < NSE 1.00	D% < ±10
Good	0.65 < NSE 0.75	±10 D% < ±15
Satisfactory	0.50 < NSE 0.65	±15 D% < ±25
Unsatisfactory	NSE 0.50	D% ±25

2.5. Modeling application

For modeling procedures, the Hydrologic Engineering Center's Hydrologic Modeling System (HEC-HMS) of the US Army Corps of Engineers (USACE) was applied [*USACE*, 2000]. HEC-HMS is designed to simulate the precipitation-runoff processes of a variety of watershed systems and applies to a wide range of hydrological problems. HEC-HMS is the most suitable platform for this study as it implements the semi-distributed ModClark Transform method, which may be coupled with grid-based loss methods. HEC-HMS is publicly available free software, and the parameters and input files for the selected models can be derived using any GIS program or using designated tools such as geoHEC-HMS for ArcGIS [*USACE*, 2013].

3 Results and discussion

The earliest DEMs were Cartographic DEMs that were derived by digitizing contours from existing topographical maps, were generally created by government agencies and commonly had resolutions of 30 or 100 meters; e.g., [*Robinson*, 1994]-[*Moore and Grayson*, 1991]. Since the late-90s, photogrammetric methods are used to obtain DEMs [*Walker and Willgoose*, 1999]. These techniques utilize aerial photograph overlapping and can obtain stereo image pairs over the same area. By the parallax effect, 3D coordinates are calculated [*Cukrov*, 2013]. The resolution of these DEMs depends on the aerial photographs' resolution and the sampling interval of the elevation points, with resolutions ranging from 0.5 meters to coarser 100-meter DEMs

The orbital RS best available DEM for the study area had a 25x25 meter resolution, which did not enable the construction of suitable DEM for hydrological modeling In this work, we have established a very detailed DEM of the Ariel watershed, using available municipal GIS data and data collected from field observations. The relevant data consisted of the following layers (Figure 2):

Vector layer of photogrammetric derived contours with a vertical interval of 0.5 meters of non-built up areas.

Vector layer of local height measurements along all the roads in the city

A road layer, including the flow direction of each road segment

Line layer of culvert location and flow direction derived from a field survey

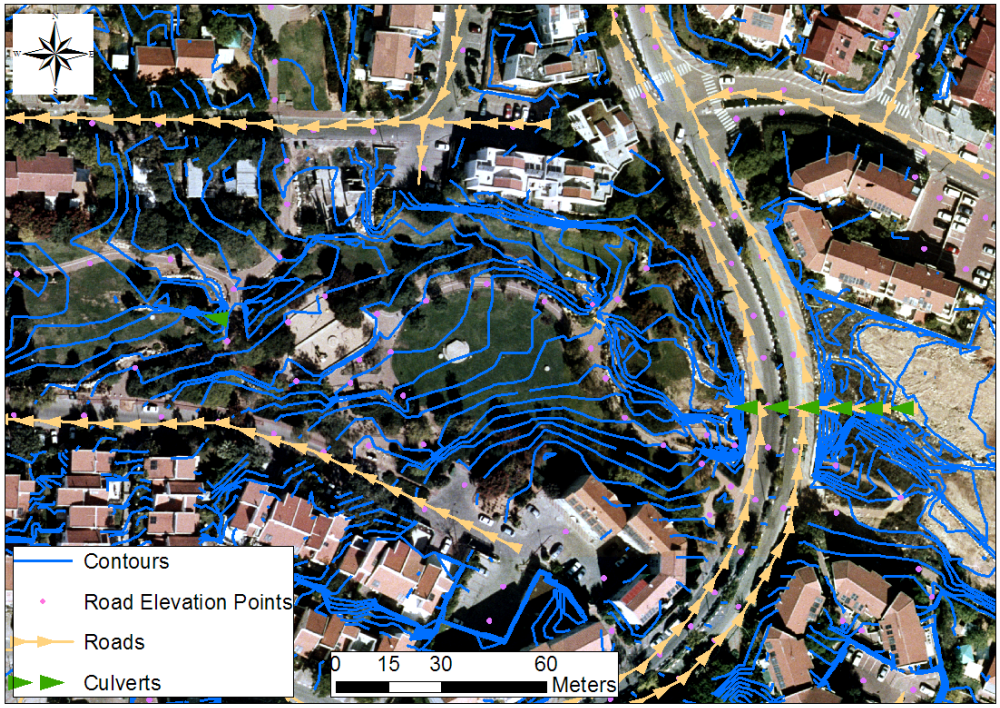

Figure 2. Part of the GIS dataset that was used for derivation of detailed DEM.

The study area is comprised of small-scale sub-watersheds in sizes ranging from 0.03 to 1.9 km^2. To enable the correct delineation of these sub-watersheds, it was necessary to evaluate the optimal DEM resolution. A few qualitative analyses were made to decide the proper DEM cell size for urban watershed delineation. DEMs were independently derived from the single GIS dataset in various cell sizes: 25-m, 10-m, 5-m, 4-m, 3-m, 2-m and 1-m. The watershed delineation procedure was done on each of the DEMs. The stream layers that were generated according to the DEMs were compared to known flow paths. DEMs with cell sizes of one to three meters were able to directly produce the flow path correctly, while DEMs of 4, 5, 10 and 25 meters failed. The lower resolution DEMs (4-m and above) indicated that the flow path of the wadi in the park was discontinued and curved north, although this is inconsistent with the observed topography and road slope.

The actual flow path continues through a culvert under the road and down to the city park's stream (Figure 3), which was derived correctly by the 1-m and 3-m DEMs. In DEMs with coarser resolution than 3-m, streamline path errors are manifested by the sub-watersheds wrong delineation. This resulted from the representation of the small-scale topography by the small cells (1-3 m) of high-resolution DEMs, which the larger cells of lower resolution DEMs (4, 5,

10, 25 m) could not capture. Since running hydrologic models in the 1-meter resolution were assumed to exceed reasonable computation time [*Vaze et al.*, 2010], there was a need to reduce the resolution and yet conserve the correct flow path and watershed boundaries.

Figure 3. Comparison of flow path delineation from DEMs that were derived directly from elevation data (contours, height points, etc.) using various cell sizes: a) and b) reproduce the actual flow path which is from east to west along the park, while c) and d) delineate a wrong north-flowing path

The basic parameters for any rainfall-runoff model are derived from the watershed's area and shape. These geometric properties control the computed runoff volume and the timing at which it will reach the outlet. The watershed area and shape delineation are derived from the watershed's topography. However, in urban watersheds, the topography is altered by man-made features such as buildings, roads and culverts. For this reason, to accurately delineate an urban watershed, high-resolution topography data is required [*Blackwell and Wells*, 1999; *Kenward et al.*, 2000; *Vaze et al.*, 2010]. Rainfall-runoff models must simulate the watershed's ability to infiltrate rain, which relates to the soil type and surface cover and also land use. While urban watersheds have heterogenic land uses with scale variation of typically a few meters, in natural watersheds the

variation of typical watershed characteristics is over a scale of tens or hundreds of meters. Urban watersheds may be hydrologically classified into impervious and pervious surfaces. Impervious surfaces prevent rainfall from infiltrating, turning practically all rainfall into surface runoff shortly after the rain starts. Pervious surfaces produce runoff in a dynamic process that may be described as a function of rainfall depth, soil type, and soil moisture conditions, among other factors [*McCuen M.*, 2004].

The most accurate DEM of 1-meter was used as the basis for derivation of coarser-resolution DEMs, indicating that the loss of details by re-sampling the higher resolution DEM to coarser resolution is much less compared to the details captured in an a priori coarse resolution DEM. Using Nearest Neighbor Interpolation (NNI), DEMs were re-sampled for selected 4-m, 10-m and 25-m cell sizes and then streets and culverts were burnt. Watershed boundaries were delineated using each of the re-sampled DEMs and were compared. The general watershed border derived using a 1-m DEM was the smoothest and described most accurately the smallest Upper-Campus sub-watershed of 0.03 km^2. DEM of 10-m and 25-m could not capture the Upper-Campus sub-watershed at all, and the general watershed border was very coarse. A comparison of the Upper-Campus sub-watershed border can be seen in Figure 4. Finally, the 4-m DEM that was produced using NNI and urban feature imprint was most similar to the 1-m DEM and it was selected to be used for hydraulic model simulation. The use of NNI and urban feature fusion to the DEM enabled using 4-m DEM instead of 3-m DEM, which was the coarser option for stream delineation at the initial assessment stage (Figure 3). Following the modeling method development for the Ariel University Campus watershed (Figure 4), the watershed analysis and flow path modeling were extrapolated to the entire city (Figure 5). This digital base layer was and still is the precise platform for performing hydrological transformation modeling that can assist the local engineering authority in drainage planning of the city of Ariel.

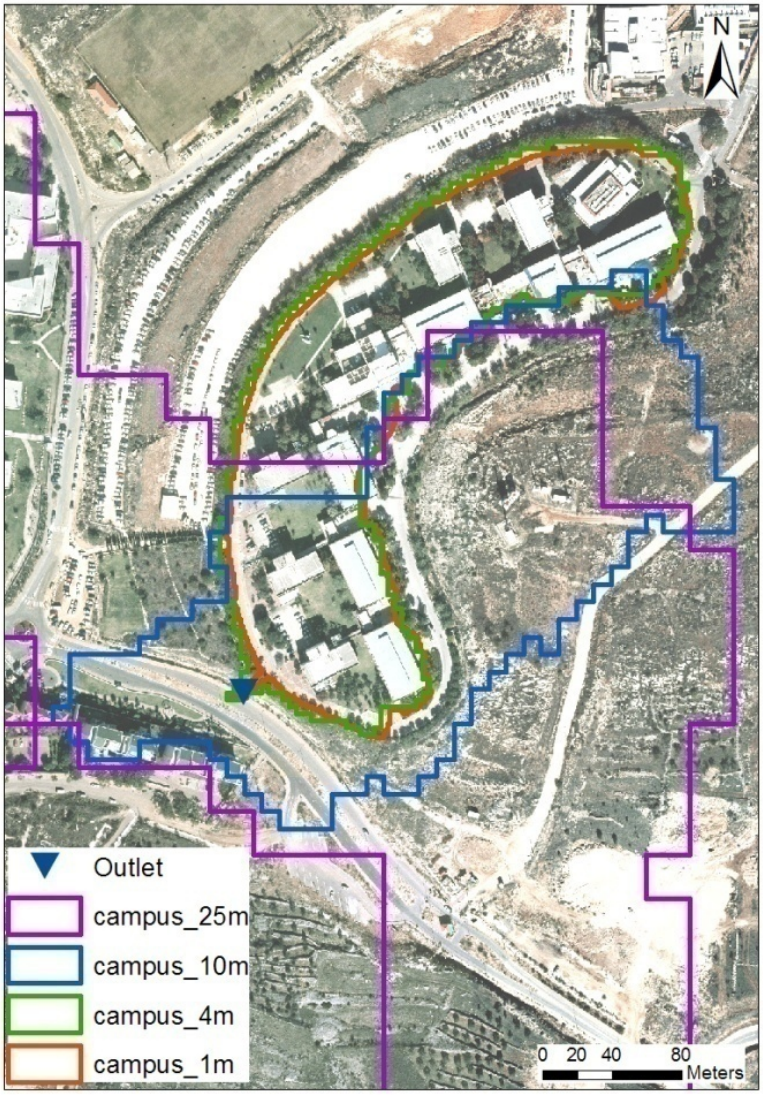

Figure 4. Comparison of Upper-Campus sub-watershed border delineated from different size DEMs

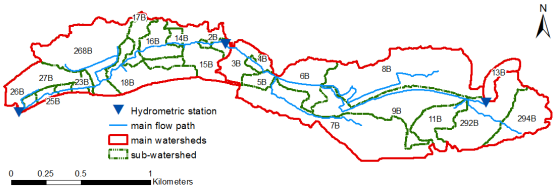

Figure 5. Sub-division of the main watersheds to sub-watersheds according to dominant flow type and streamline pathways.

There are many techniques to automatically classify land cover information from remotely sensed satellite imagery, with the aid of GIS. Traditional classification methods use typical reflectance characteristics of relevant land covers and various pixel-by-pixel classification algorithms such as Maximum Likelihood Classifier (MLC), to assign each pixel to the land cover class that it best matches. However, some acknowledged weaknesses when mapping urban areas using pixel-by-pixel classification algorithms are the imperfect differentiation of some anthropogenic surfaces such as concrete from soil features [*Myeong et al.*, 2001]. Important semantic/spatial information required to interpret the image is not accounted for by these algorithms Other classification approaches are supplied by the image-segmentation techniques which are often advantageous when high-resolution data is used. These algorithms make use of both spectral and spatial information and generate pixel groups (clusters), which are spectrally homogeneous and recognizable as segments of a landscape. This method has been successfully applied for high-resolution classification [*Thomas et al.*, 2003].

In this work, advanced GIS and Remote Sensing techniques including feature-based segmentation were employed to generate high-resolution LU/LC classification in a semi-automated way. A segmentation level value of 31 and a merging level value of 91 was found best for individual delineation of roads (Fig. 6), buildings, groves, and lawns, as can be seen in Figures 6 & 7 . In natural open areas where the land cover consists of patches of bare soil, rocks and shrubs - the segmentation process delineated each of these objects separately as they have different properties (Figure 7). In post-classification processes, these objects are merged into more general classes.

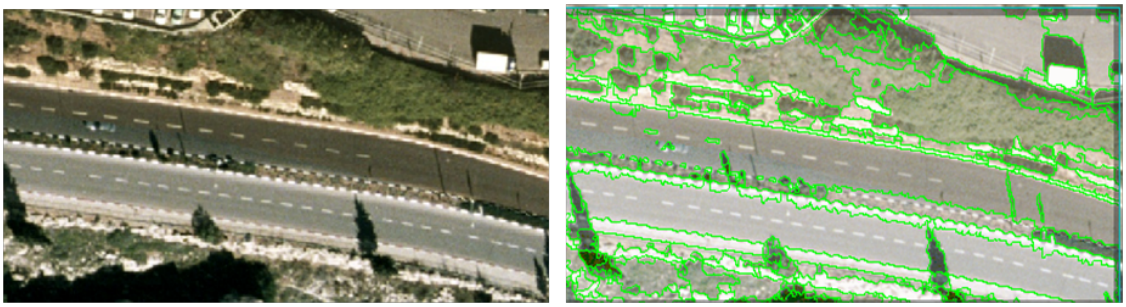

Figure 6. Delineation of urban objects using feature extraction module with segmentation and merging processes.

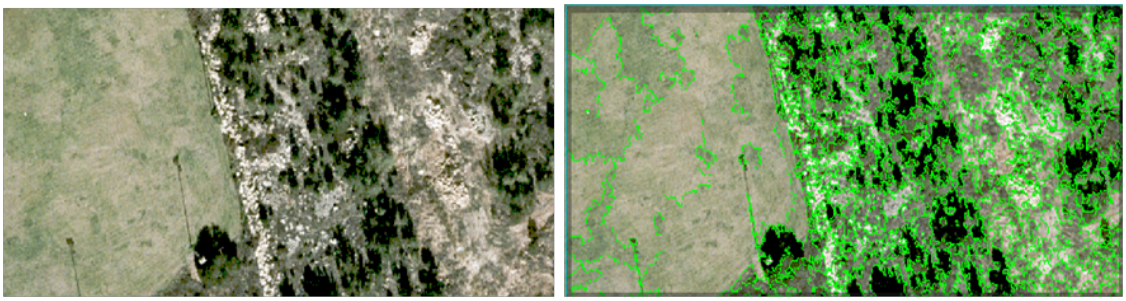

Figure 7. The left image shows a patch of lawn and an adjacent natural open area. The right image shows detailed segmentation of the open area due to the many different objects within it.

To get accurate classification, as many as 13 classes were defined. This high number of classes is important to distinguish between features of one LU type that have many different appearances (for example, red roof, gray roof, and road are three different classes that are classified, and later merged into a single impervious area LU class). A training dataset is prepared by a manual selection of objects that belong to each class. Supervised classification is then performed on the entire image using the training data. The K-Nearest Neighbor (KNN) method is used with K=3. The feature extraction procedure is run on the separated shaded areas, and they are classified as LU as well.

A post-processing stage included manual correction of classification errors using vector GIS data. Buildings that were classified wrongly as the open area were changed to impervious using intersection with the building layer, while open area patches that were wrongly classified as impervious were changed into bare soil. The manual correction served as a tool for validating the classification results.

Ultimately, a LU classification map was created, containing five LUs: Impervious surfaces, Lawns, Groves, Bare soil and Limestone (Figure 8). The original classified map is of 0.2 m resolution and was resampled to the selected model

cell size of 4 meters. The flow chart in Appendix B describes the preparation of LU/LC classification as part of the total model implementation methodology.

Figure 8. Land Use map, derived from high-resolution orthophoto in a feature extraction-based classification process.

Following the hydrological setting delineation, the modeling procedure integrated several models including SCS-CN, ModClark and Muskingum-Cunge, which were needed to quantify the parameters for the runoff modeling (Table 2).

Table 2: a list of model parameters for the selected components of the model

@ >p(- 2) * >p(- 2) * @ **Model** & **Parameter Name**
SCS-CN loss method &

- Curve Number (CN)

ModClark transformation method &

- Time of Concentration (Tc)

&

- Storage coefficient (R)

Muskingum-Cunge routing method &

Cross-section parameters:

- length,
- slope,
- Manning's N,
- bottom width,
- side slope,
- diameter (for pipes).

&

- Percolation rate (K)

The CN, Tc and Cross-section parameters were estimated based on various measurable physical properties of the watershed and were derived using DEM, LU/LC classification, field surveys and precipitation data. The other parameters - Storage coefficient (R) and Percolation rate (K) - were calibrated using measured rainfall and runoff data [*USDA*, 1986]. Figure 9 is a flow chart that represents the possible modeling combinations, according to the estimation of each model parameter as part of the total model implementation methodology.

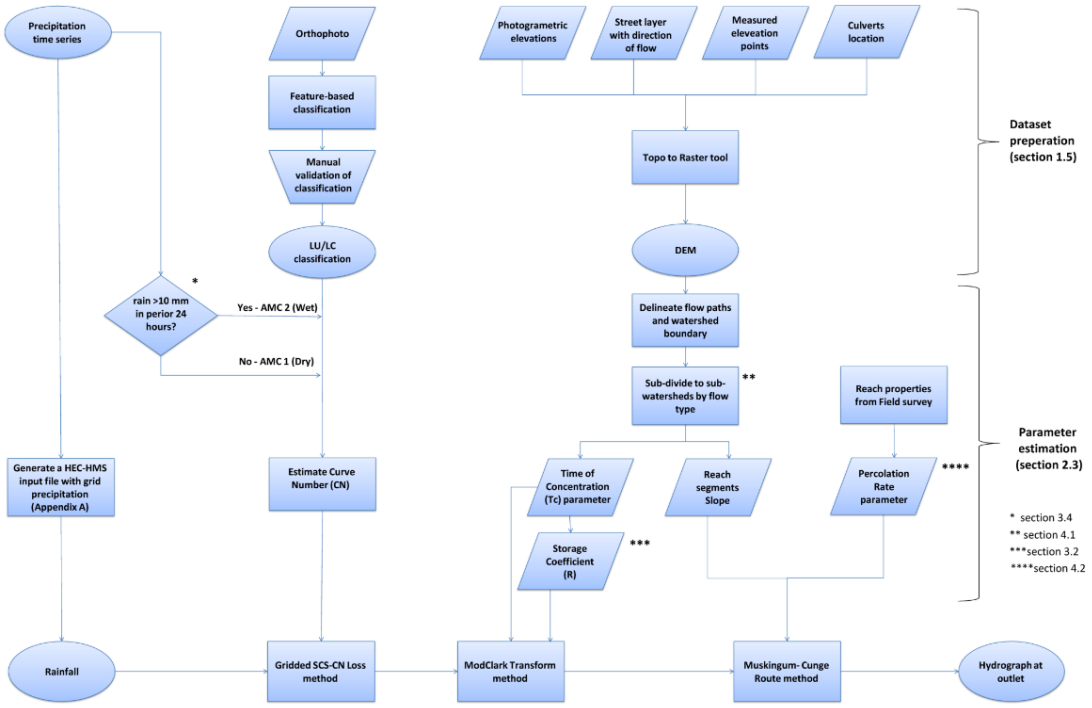

Figure 9. Flow chart of the modeling procedure.

Following a model training stage, seven rain events were used for the model calibration. Rain events were defined as follows: a rain event starts with the beginning of rainfall provided that the measured discharge was zero for at least four hours before the rain started; an event ends after the rainfall ceased and only when the discharge equals or tends to zero in all hydrometric stations. The Storage Coefficient value, R, was determined through calibration. The value of R was changed manually within a reasonable range until a satisfactory agreement was obtained between the observed and simulated hydrographs.

Figure 10 shows observed versus simulated hydrographs for selected events; all other event hydrographs can be found in Appendix D. Visual inspection of the simulated and observed hydrographs shows a good correlation in the timing of peaks.

[CHART]

[CHART]

[CHART]

Figure 10. Calibration results showing simulated versus observed hydrographs and precipitation for selected events.

The calibration process resulted in a good fit to the observed values, which were evaluated using three statistical indicators: NSE coefficient, runoff depth deviation percent and peak discharge deviation percent (as described in section 2.3.7). The calibrated event properties and performance statistics are summarized in Table 11. Comparison of the fit of the simulated and observed hydrographs using the NSE coefficient gave satisfactory to very good performance with NSE in the range of 0.62-0.95. The performance indicated by runoff depth D% is rated good to satisfactory with a range of -12.91% to +32.08%.

As the events have multiple peaks, the peak discharge deviation percent compares the highest observed peak to the simulated peak of the same time. The peak discharge deviation percent ranged from -35% to -4%.

4 Conclusions

The optimal resolution for implementing a grid-based model for the Ariel urban watershed was derived as four meters: DEM of the lower resolution was unable to indicate the urban flow paths or to accurately delineate the watershed border while using DEM of higher resolution might increase the computation time of the model. The integration of NNI DEM resampling and urban feature fusion enabled the use of 4-m DEM instead of 3-m DEM, and the city digital base layer that was produced enabled the correct modeling of urban runoff of the city of Ariel as representative of mountainous urban karstic terrain.

The results indicate that the best performance was obtained when R=0.2 (hr.), with very minor deviations from it. Thus, a relationship between R and t_c was derived as follows:

R=2*t_c Eq. 4

This relationship was used to derive R values for every other sub-watershed in this study.

The optimized DEM watershed sub-division and land use classification improved the model's performance as the sub-division simulation hydrographs and the test simulation was like the observed hydrographs (Figure 11).

[CHART][CHART]

Figure 11. Simulated and observed runoff properties for the Sheshet watershed.

Applying an optimal resolution to a hydrological instead of the highest available resolution has several advantages. Besides the evident reduction in computer resources, the lower resolution acts as a smoothing filter that prevents the bias from minor structural elements that do not influence real-world hydrology. The model performed in a representative mountainous karstic urbanized area was found to concur with the actual measurements and with minor alignments, may be applied to similar regions worldwide.

Acknowledgments

This study was supported by the Israeli Ministry of Science and Technology (grant number). The continuation of this study is done within the framework of the GRaCCE project as a subcontractor of the Ben Gurion University, with Prof. Noam Weisbord as PI (contract # 3-17770). The authors would also wish to thank the Ariel city Engineering Department for supplying a high-resolution orthophoto, city measurements and other useful GIS data and to eng. Alexander Gimburg for preforming the filed operation.

Open Research

The data and detailed description of the procedures presented in this paper are available at: Rainfall-Runoff model for mountainous karst urban watersheds in Israel Case study: City of Ariel - Mendeley Data

References

Anker, Y., Y. Hershkovitz, E. Ben Dor, and A. Gasith (2014), Application of aerial digital photography for macrophyte cover and composition survey in small rural streams, *River Res. Appl.*, *30*(7), doi:10.1002/rra.2700.Anker, Y., V. Mirlas, A. Gimburg, M. Zilberbrand, F. Nakonechny, I. Meir, and M. Inbar (2019), Effect of rapid urbanization on Mediterranean karstic mountainous drainage basins, *Sustain. Cities Soc.*, *51*(February), 101704, doi:10.1016/j.scs.2019.101704. [online] Available from: https://linkinghub.elsevier.com/retrieve/pii/S22106707
P., and G. Wells (1999), DEM Resolution and Improved Surface Representation, *ESRI Proc.* [online] Available from: http://proceedings.esri.com/library/userconf/proc99/proceed/papers/pap
(Accessed 26 January 2020)Branger, F., S. Kermadi, C. Jacqueminet, K. Michel, M. Labbas, P. Krause, S. Kralisch, and I. Braud (2013), Assessment of the influence of land use data on the water balance components of a peri-urban catchment using a distributed modelling approach, *J. Hydrol.*, *505*, 312–325, doi:10.1016/j.jhydrol.2013.09.055. [online] Available from: http://dx.doi.org/10.1016/j.jhydrol.2013.09.055Cukrov, G. (2013), Using Stereo Photogrammetry to Create Digital Elevation Models of Planetary Surfaces, *2013 Ncur*, *0*(0), 1–4. [online] Available from: http://www.ncurproceedings.org/ojs/index.php/NCUR2013/article/view/585Dan, Y., Z. Raz, H. Yaalon, and H. . Koyumdjisky (1995), Soil Map of Israel, *Surv. Isr.*Fletcher, T. D., H. Andrieu, and P. Hamel (2013), Understanding, management and modelling of urban hydrology and its consequences for receiving waters: A state of the art, *Adv. Water Resour.*, *51*, 261–279, doi:10.1016/J.ADVWATRES.2012.09.001. [online] Available from: https://www.sciencedirect.com/science/article/abs/pii/S0309170812002412?via%3Dihub#!
(Accessed 26 January 2020)Fohrer, N., S. Haverkamp, K. Eckhardt, and H. G. Frede (2001), Hydrologic response to land use changes on the catchment scale, *Phys. Chem. Earth, Part B Hydrol. Ocean. Atmos.*, *26*(7–8), 577–582, doi:10.1016/S1464-1909(01)00052-1.Gao, J., Y. Jiang, and Y. Anker (2021), Contribution analysis on spatial tradeoff/synergy of Karst soil conservation and water retention for various geomorphological types: Geographical detector

application, *Ecol. Indic.*, *125*, 107470, doi:10.1016/j.ecolind.2021.107470. [online] Available from: https://doi.org/10.1016/j.ecolind.2021.107470Gironás, J., L. a. Roesner, L. a. Rossman, and J. Davis (2010), A new applications manual for the Storm Water Management Model (SWMM), *Environ. Model. Softw.*, *25*(6), 813–814, doi:10.1016/j.envsoft.2009.11.009. [online] Available from: http://linkinghub.elsevier.com/retrieve/pii/S1364815209002989 (Accessed 3 August 2010)Greenlee, D. D. (1987), Raster and vector processing for scanned linework, *Photogramm. Eng. Remote Sens.*, *53*(10), 1383–1387.Gupta, H. V., S. Sorooshian, and P. O. Yapo (1999), Status of Automatic Calibration for Hydrologic Models: Comparison with Multilevel Expert Calibration, *J. Hydrol. Eng.*, *4*(2), 135–143, doi:10.1061/(asce)1084-0699(1999)4:2(135).Gvirtzman, H. (2002), *Israel Water Resources*, 1st ed., Yad Ben-Zvi Press, Jerusalem.Hankin, B., S. Waller, G. Astle, and R. Kellagher (2008), Mapping space for water: screening for urban flash flooding, *J. Flood Risk Manag.*, *1*(1), 13–22, doi:10.1111/j.1753-318x.2008.00003.x.Hutchinson, M. F. (1989), A new procedure for gridding elevation and stream line data with automatic removal of spurious pits, *J. Hydrol.*, *106*(3–4), 211–232, doi:10.1016/0022-1694(89)90073-5. [online] Available from: https://www.sciencedirect.com/science/article/pii/0022169489900735 (Accessed 26 January 2020)Jacobson, C. R. (2011), Identification and quantification of the hydrological impacts of imperviousness in urban catchments: A review, *J. Environ. Manage.*, *92*(6), 1438–1448, doi:10.1016/j.jenvman.2011.01.018.Jacqueminet, C., S. Kermadi, K. Michel, D. Béal, M. Gagnage, F. Branger, S. Jankowfsky, and I. Braud (2013), Land cover mapping using aerial and VHR satellite images for distributed hydrological modelling of periurban catchments: Application to the Yzeron catchment (Lyon, France), *J. Hydrol.*, *485*, 68–83, doi:10.1016/j.jhydrol.2013.01.028. [online] Available from: http://dx.doi.org/10.1016/j.jhydrol.2013.01.028Jenson, S. K., and J. O. Domingue (1988), Extracting topographic structure from digital elevation data for geographic information system analysis, *Photogramm. Eng. Remote Sensing*, *54*(11), 1593–1600.Jiao, L., Y. Liu, and H. Li (2012), Characterizing land-use classes in remote sensing imagery by shape metrics, *ISPRS J. Photogramm. Remote Sens.*, *72*, 46–55, doi:10.1016/j.isprsjprs.2012.05.012. [online] Available from: http://dx.doi.org/10.1016/j.isprsjprs.2012.05.012Kenward, T., D. P. Lettenmaier, E. F. Wood, and E. Fielding (2000), Effects of Digital Elevation Model Accuracy on Hydrologic Predictions, *Remote Sens. Environ.*, *74*(3), 432–444, doi:10.1016/S0034-4257(00)00136-X. [online] Available from: https://linkinghub.elsevier.com/retrieve/pii/S003442570000136X (Accessed 26 January 2020)Legates, D. R., and G. J. McCabe (1999), Evaluating the use of "goodness-of-fit" measures in hydrologic and hydroclimatic model validation, *Water Resour. Res.*, *35*(1), 233–241, doi:10.1029/1998WR900018.Lhomme, J., C. Bouvier, and J.-L. Perrin (2004), Applying a GIS-based geomorphological routing model in urban catchments, *J. Hydrol.*, *299*(3–4), 203–216, doi:10.1016/j.jhydrol.2004.08.006.Litvak, I., Y. Anker, and H. Cohen (2018), In-Situ Measurements of Carbon Stable Isotopes Ratio in Karstic Caves by FTIR Spectroscopy, *Int. J. Chem.*

Eng. Appl., *9*(3), 101–106, doi:10.18178/ijcea.2018.9.3.707.Mark, O., S. Weesakul, C. Apirumanekul, S. B. Aroonnet, and S. Djordjević (2004), Potential and limitations of 1D modelling of urban flooding, *J. Hydrol.*, *299*(3–4), 284–299, doi:10.1016/J.JHYDROL.2004.08.014. [online] Available from: https://www.sciencedirect.com/science/article/pii/S0022169404003737 (Accessed 27 January 2020)McCuen M., R. (2004), *Hydrologic Analysis and Design, 3rd edition*, Prentice-Hall. [online] Available from: https://books.google.co.il/books/about/Hydrologic_analysis_and_design.html?id=9PZRAAAAMAAJ&redir (Accessed 26 January 2020)Moore, I. D., and R. B. Grayson (1991), Terrain-based catchment partitioning and runoff prediction using vector elevation data, *Water Resour. Res.*, *27*(6), 1177–1191, doi:10.1029/91WR00090. [online] Available from: http://doi.wiley.com/10.1029/91WR00090 (Accessed 27 January 2020)Moriasi, D. N., M. W. Arnold, M. W. Van Liew, R. L. Bingner, R. D. Harmel, and T. L. Veith (2007), MODEL EVALUATION GUIDELINES FOR SYSTEMATIC QUANTIFICATION OF ACCURACY IN WATERSHED SIMULATIONS, *Am. Soc. Agric. Biol. Eng.*, *39*(3), 227–234.Murphy, P. N. C., J. Ogilvie, F.-R. Meng, and P. Arp (2008), Stream network modelling using lidar and photogrammetric digital elevation models: a comparison and field verification, *Hydrol. Process.*, *22*(12), 1747–1754, doi:10.1002/hyp.6770. [online] Available from: http://doi.wiley.com/10.1002/hyp.6770 (Accessed 27 January 2020)Myeong, S., D. Nowak, P. Hopkins, and R. Brock (2001), Urban cover mapping using digital, high-spatial resolution aerial imagery, *Urban Ecosyst.*, *5*(4), 243–256, doi:10.1023/A:1025687711588.Nash, J. E., and J. V. Sutcliffe (1970), River flow forecasting through conceptual models part I - A discussion of principles, *J. Hydrol.*, *10*(3), 282–290, doi:10.1016/0022-1694(70)90255-6.Ne'eman, N. (2015), Rainfall-Runoff model for mountainous karst urban watersheds in Israel Case study : City of Ariel Nitzan Ne ' eman Rainfall-Runoff model for urban watersheds in Israel Case study : City of Ariel, Tel Aviv University.Olivera, F., and D. Maidment (1999), Model for Runoff Routing, *Water Resour. Res.*, *35*(4), 1155–1164. [online] Available from: http://www.sciencedirect.com/science/article/pii/0022169464900253Robinson, G. J. (1994), THE ACCURACY OF DIGITAL ELEVATION MODELS DERIVED FROM DIGITISED CONTOUR DATA, *Photogramm. Rec.*, *14*(83), 805–814, doi:10.1111/j.1477-9730.1994.tb00793.x. [online] Available from: http://doi.wiley.com/10.1111/j.1477-9730.1994.tb00793.x (Accessed 27 January 2020)Rodriguez, F., H. Andrieu, and Y. Zech (2000), Evaluation of a distributed model for urban catchments using a 7-year continuous data series, *Hydrol. Process.*, *14*(5), 899–914, doi:10.1002/(SICI)1099-1085(20000415)14:5<899::AID-HYP977>3.0.CO;2-R. [online] Available from: http://doi.wiley.com/10.1002/%28SICI%291099-1085%2820000415%2914%3A5%3C899%3A%3AAID-HYP977%3E3.0.CO%3B2-R (Accessed 27 January 2020)Tarboton, D. G., R. L. Bras, and I. Rodriguez-Iturbe (1991), On the extraction of channel networks from digital elevation data, *Hydrol. Process.*, *5*(1), 81–100, doi:10.1002/hyp.3360050107.Thomas, N., C. Hendrix, and R. G. Congalton (2003), Urban Mapping Methods, *Photogramm. Eng. Remote Sens.*, *69*(9), 963–972.USACE (2000), *Hydrologic Model-*

*ing System.*USACE (2013), *HEC-GeoHMS 10.1 Geospatial Hydrologic Modeling Extension.* [online] Available from: http://www.hec.usace.army.mil/software/hec-geohms/documentation/HEC-GeoHMS_Users_Manual_10.1.pdfUSDA (1986), *Urban Hydrology for Small.* [online] Available from: http://scholar.google.com/scholar?hl=en&btnG=Se J., J. Teng, and G. Spencer (2010), Impact of DEM accuracy and resolution on topographic indices, *Environ. Model. Softw.*, *25*(10), 1086–1098, doi:10.1016/J.ENVSOFT.2010.03.014. [online] Available from: https://www.sciencedirect.com/science/article/pii/S1364815210000733 (Accessed 26 January 2020)Walker, J. P., and G. R. Willgoose (1999), On the effect of digital elevation model accuracy on hydrology and geomorphology, *Water Resour. Res.*, *35*(7), 2259–2268, doi:10.1029/1999WR900034.Zech, Y., X. Sillen, C. Debources, and A. Van Hauwaert (1994), Rainfall-runoff modelling of partly urbanized watersheds: Comparison between a distributed model using GIS and other models sensitivity analysis, in *Water Science and Technology*, vol. 29, pp. 163–170.

Figure 1. The figure caption should begin with an overall descriptive statement of the figure followed by additional text. They should be immediately after each figure. Figure parts are indicated with lower-case letters (a, b, c...). For initial submission, please place both the figures and captions in the text near where they are cited rather than at the end of the file (not both). At revision, captions can be placed in-text or at the end of the file, and figures should be uploaded separately. Each figure should be one complete, cohesive file (please do not upload sub-figures or figure parts in separate files). Data that supports the figure must be preserved in a repository, included in the Open Research section, and cited in the References. Include detailed information on how to recreate the figure in support of transparency (e.g., Python, R library).

Table 1. Start this caption with a short description of your table. Format tables using the Word Table commands and structures. Additional information on table formatting can be found in our Style Guide, Table Formatting. Do not create tables using spaces or tab characters. Large tables should not be included in the main text of the paper, but instead preserved as a .csv file in a repository. All data displayed in tables must be preserved in a repository, included in the Open Research section, and cited in the References.

Figure 1. The figure caption should begin with an overall descriptive statement of the figure followed by additional text. They should be immediately after each figure. Figure parts are indicated with lower-case letters (**a, b, c...**). For initial submission, please place both the figures and captions in the text near where they are cited rather than at the end of the file (not both). At revision, captions can be placed in-text or at the end of the file, and figures should be uploaded separately. Each figure should be one complete, cohesive file (please do not

upload sub-figures or figure parts in separate files).

Table 1. Start this caption with a short description of your table. Format tables using the Word Table commands and structures. Additional information on table formatting can be found in our Style Guide, Table Formatting. Do not create tables using spaces or tabs characters. Large tables presenting rich data should be presented as separate excel or .csv files, not as part of the main text.